Journal homepage www.jzs.univsul.edu.iq
Journal of Zankoy Sulaimani
Part-A- (Pure and Applied Sciences)

Seismicity, Velocity Structure and Tectonics of the Arabian Plate

Hafidh A. A. Ghalib[1] & Ghassan I. Aleqabi[2]

1 Array Information Technology, 5130 Commercial Drive, Suite B, Melbourne, FL 32940, USA, e-mail: hafidh.ghalib@arrayinfotech.com
2 Washington University in Saint Louis, Campus Box 1169, One Brookings Drive, Saint Louis, MO 63130, USA, e-mail: ghassan@mantle.wustl.edu

Article info

Original: 06.10.2015
Revised:14.06.2016
Accepted:16.06.2016
Published online: 01.07.2016

Key Words:
Arabian Plate
Seismicity
Velocity Structure
Source Mechanism

Abstract

The deployment of the North Iraq Seismographic Network (NISN) and of the array KSIRS and the implementation of the virtual Middle East Seismographic Network (vMESN) produced a wealth of unprecedented data for use in studying the seismicity, velocity structure and some aspects of the tectonic activities associated with the Arabian plate dynamics. Recent studies using stationary Global Positioning System (GPS) stations in the region clearly show the northeast trending transitional and counterclockwise rotational motions of the plate. Most of the seismicity is occurring in the crust along the Zagros and Taurus mountain ranges and their foothills, along the Dead Sea transform fault and along the rift zones in the Red Sea and the Gulf of Aden. Earthquakes with magnitude greater than 5 m_b are not frequent. Likewise, intermediate and deep earthquakes are uncommon in the region. The great majority of the earthquakes occur as a result of the continental collision between the Arabian plate and the Iranian and Turkish plateaus. Preliminary analysis of the earthquakes' spatial distribution suggests likely alignment with the faults in the region. Moment tensor analysis of the larger events, carried out as part of the routine data processing, suggests their focal mechanisms vary from normal, reverse to strike-slip depending on the local stress pattern and the event's location relative to the Zagros and Taurus suture zones. The three-dimensional crustal seismic velocity structure of the Arabian plate and surrounding regions estimated from the dispersion of Rayleigh surface waves reflects the impact of the overlying 5-10 km thick sedimentary column on the morphology of the crystalline basement, the Conrad and Moho discontinuities whose depths range from 20-25 km and 40-50 km, respectively. The teleseismic P-wave receiver function analysis provided an independent verification of the velocity models beneath the various stations used in the study of the region. In summary, the resulting models show remarkable correlation between the distribution of shear velocities and the major physiographic and tectonic provinces of the Arabian plate, Turkish and Iranian plateaus. It also helped delineate the extent of the Red Sea rift and the roots of the Zagros and Taurus mountain ranges.

Introduction

The Arabian plate is comprised of diversified seismotectonic environments. Its boundaries are associated with seismically active zones consisting of continental collision, sea-floor spreading, transform faulting and subduction. The plate's major tectonic provinces include the Arabian shield and platform, the Mesopotamian

foredeep and the Zagros folded belt. A large portion of this relatively young, intensely faulted and metamorphosed shield is exposed to the surface. The folded belt and most of the foredeep include very thick sedimentary layers from the time of the Tethys Ocean. Folding and faulting are extensive throughout the entire plate. In addition, evidence of recent volcanic activity can be found along the plate's western boundary parallel to the Red and Dead Seas. Although interplate earthquakes are more frequent than intraplate events, through the centuries various regions of the plate have experienced devastating moderate to large earthquakes. Historical manuscripts are rich with descriptive accounts of many such catastrophic earthquakes.

Nevertheless, the Arabian plate is probably still one of the least studied seismotectonic regions of the Earth. In particular, very little is known about the variation of both its crustal and upper mantle velocity structures or about attenuation of seismic waves within such a relatively large lithospheric block. In past decades, only a limited number of local and regional studies attempting to explain the physical or structural features of this plate have been published. In general, most of our present knowledge of the region has evolved from geological and shallow geophysical exploration surveys. It is unfortunate that research on the seismotectonics of the plate has not been fully supported, since it can also provide economic benefits. The information this research contributes is necessary for a variety of purposes, including the investigation of seismic waves propagation, locating earthquakes, developing local magnitude relations, assessment and mitigation of earthquake risk, and interpreting the composition and evolution of the plate.

The objective of this study is to investigate the characteristics and structure of the crust in the region through the analysis of long-period Rayleigh and teleseismic body waves.

Tectonic Framework

The Arabian plate is surrounded by the African plate to the west and south and by the Turkish and Iranian plateaus to the north and east (*Figure: 1*). Geologically, the Arabian plate is characterized by diversified physiographic and tectonic environments. The research published by *[1, 2]*, among many other investigators, provide detailed reviews and discussions of the seismotectonic framework of the Arabian plate. Hence, only a brief description of the tectonic setting that is relevant to this study is presented herein.

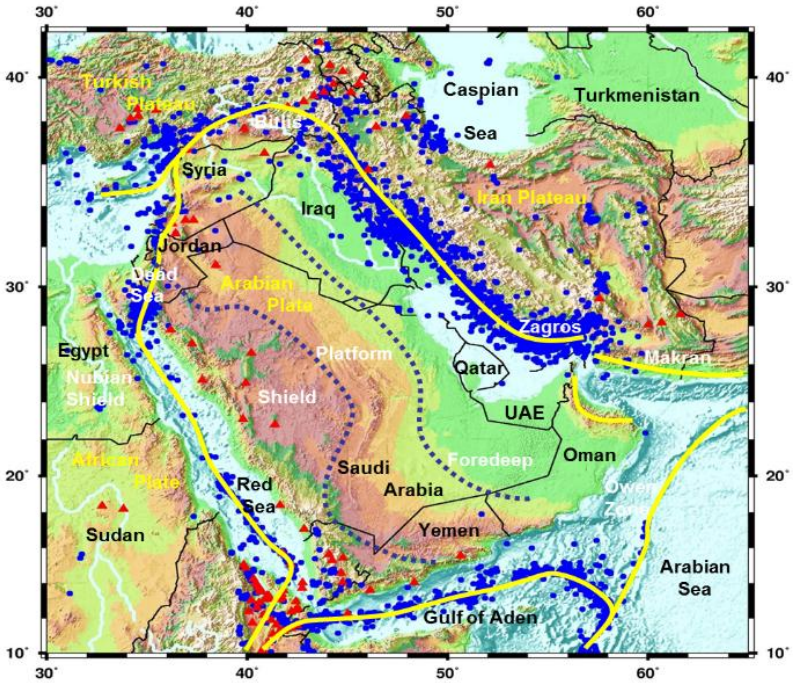

Figure-1: Map showing the seismotectonic framework of the Arabian plate; boundaries (yellow solid lines), seismicity (blue dots) and volcanoes (red triangles). It also shows the major physiographic zones of the plate (*i.e.*, Arabian shield, platform and foredeep).

The Taurus/Bitlis and Zagros continental collision zones form the northern, northeastern and eastern boundaries of the Arabian plate. They are the result of continued convergence between the Arabian plates and the Turkish and Iranian plateaus. The Taurus zone is diffused, but the Zagros is well defined and extends for about 1500 km in a NW-SE direction. The structural deformation of these zones probably dates back to the Mesozoic and Miocene times *[3, 4]*. The main thrust zone of these orogenic zones is flanked to the south and southwest by a simple folded belt that extends well into the Mesopotamian foredeep. Presumably this belt is present because there are thick (more than 1 km) plastic salt beds that decouple the sedimentary column from the basement of the plate *[5, 6]*. Faults are relatively scarce within the thick (5-10 km) sediments of this belt, and they are mainly restricted to the Precambrian basement, *e.g.*, *[7, 8, 9, 10, 11]*.

The southern and southwestern boundaries of the Arabian plate are defined by active sea floor spreading in the Gulf of Aden and the Red Sea, respectively, *e.g.*, *[12, 13, 14, 15, 16, 17]*. The structure of the Gulf of Aden is characterized by an E-W trending main axial trough of regional expansion, whereas a main trough and axial troughs, which were developed during the Oligocene through Pliocene, characterize the structural features of the Red Sea. In addition, many NE-SW trending transform faults are known to intersect the oceanic trough of these major rift systems.

The northwestern margin of the Arabian plate is defined by the Dead Sea transform fault system, *e.g.*, *[18, 19, 20, 21, 22, 23, 24]*. This N-S trending plate boundary, which was developed in multiple stages during the Middle Cenozoic, extends from the Red Sea to the Taurus convergence zone. Although the predominant motion along the Dead Sea is left-lateral strike-slip, it is also considered a leaky transform system due to the existence of lateral extension and compression stress components and up-warping along the fault caused by the divergence between the Arabian and African plates.

The physiographic regions of the plate feature a relatively young metamorphosed Arabian shield, a transitional platform zone, and a foredeep of thick sediments. The Arabian shield occupies approximately a third of the total area of the Arabian plate, and it runs parallel to the eastern coast of the Red Sea. Its exposed Precambrian rocks consist of complex metamorphic, plutonic, magmatic and ophiolitic assemblages. Thin basaltic lava flows cover vast areas of the shield since the Miocene time. These reflect the intensity of historic volcanism in the region *[25]*. Further evidence of the tectonic activity level is reflected by the abundance of major NW trending normal and strike-slip type faults *[26]*.

The Arabian platform and Mesopotamian foredeep occupy the other two thirds of the plate. The Phanerozoic platform region is relatively stable, and it consists of Paleozoic and Mesozoic sedimentary layers. The thickness of sediments increases toward the east and northeast following the gradual dip of the basement in those directions. Neither near-surface faults nor folds are common within the vast platform region. In contrast, the Mesopotamian foredeep, which marks the location of the Tethys geosyncline, is characterized by significantly increased thickness of sediments and structural deformation. The column of sediments in various parts of this region exceeds 10 km, and it is presumably separated from the basement by thick salt deposits *[5]*. The intensity of folding in the foredeep increases toward the northern, northeastern and eastern boundaries of the Arabian plate. In most cases the folds, which date back to the Upper Miocene-Lower Pliocene *[7]*, run parallel to the extension of the Taurus and Zagros mountains. Furthermore, strike-slip, reverse and normal faults are also more common in the foredeep than in the platform region.

Seismicity

Figure: 2 shows the motion of the Arabian plate relative to the African and Eurasian plates. Global Positioning System (GPS) derived velocity field (1988–2005) measurements indicate counterclockwise rotation of a broad area of the Earth's surface including the Arabian plate, adjacent parts of the Zagros, and central Iran and Turkey relative to Eurasia at rates in the range of 20–30 mm/yr *[27, 28]*. As a result, most of the seismicity is interplate and is associated with the tectonic activity along the boundaries of the plate, including the foothills of the Taurus/Bitlis and Zagros folded belts, whereas intraplate earthquakes are infrequent and rarely exceed magnitude 4.5 m_b.

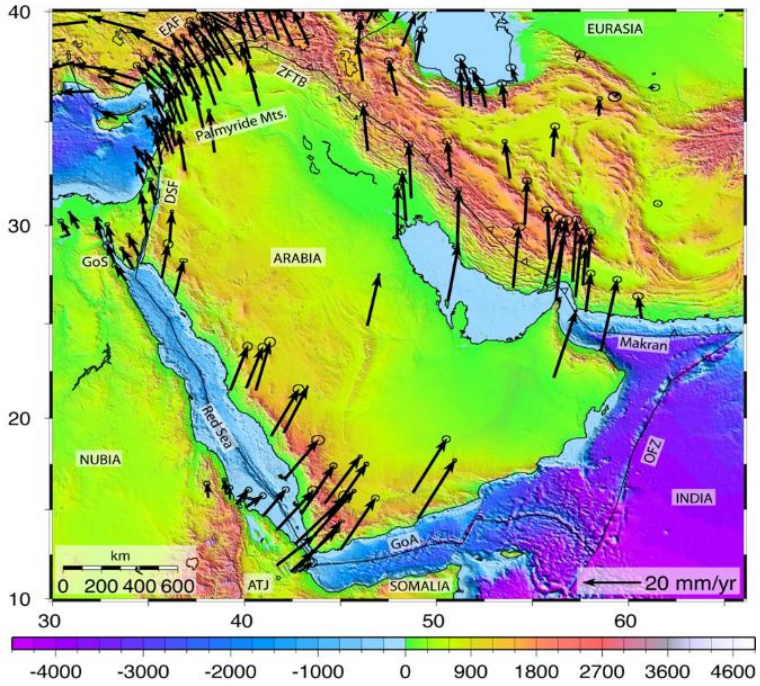

Figure-2: Map showing counterclockwise rotation of the Arabian plate determined from GPS velocities relative to Eurasia *[27, 28]*.

Since the establishment of North Iraq Seismographic Network (NISN) in 2006 *[29]*, a wealth of high quality three-component broadband waveform data has been collected and analyzed. *Figure: 3* shows a composite seismicity map of the Arabian plate and surrounding regions for the period 1905-2015 according to the US Geological Survey (USGS) National Earthquake Information Center (NEIC). In this figure the location of these 12604 undifferentiated events is depicted in solid gray colored circles. They are included to delineate the boundaries of the Arabian plate (along the Dead Sea, Red Sea and Gulf of Eden, in particular) and the seismicity in the neighboring countries, *i.e.*, Turkey and Iran. *Figure: 3* is "composite" because this version of the Middle East (ME) seismicity map also shows the 8015 earthquakes that were located using the NISN seismic phases onset times augmented with those reported in the Turkish, Iranian, NEIC bulletins. A much more comprehensive picture of the region's seismicity would emerge if data from the abundant seismic stations in all of the ME countries were to be incorporated into the process of detecting and locating the earthquakes *[30, 31, 32]*. For example, if data from the networks in Jordan, Syria and Lebanon were to be shared and included in the analysis, earthquakes along the Dead Sea Transform Fault would be much better delineated than is shown in *Figure: 3*. Also, if data from the networks in Saudi Arabia, Yemen, Oman and United Arab Emirates, Qatar and Kuwait were to be shared and included in the analysis, the seismicity along the Red Sea, the Gulf of Adan and the Arabian Sea would be much better delineated. Moreover, including all of these data would greatly help delineating the Arabian intraplate seismicity better than is shown in *Figure: 3*. It is well understood that detecting, precisely locating, and estimating the depth and magnitude of an earthquake depends not only on the number of stations recording it but also on the azimuthal distribution of the stations around the event. It is also well understood that advanced analytical techniques (*e.g.*, Moment Tensor and Receiver Function analysis) require waveforms recorded at stations with favorable azimuthal coverage and varying epicentral distances.

In *Figure: 3* the NISN events are distinguished by their hypocentral depth (solid colored circles) and their duration magnitude (circle size). The events are located using the Zagros fold and thrust zone model *[33]*. Despite the fact that estimating the precise depth of an earthquake requires extensive data from local and

regional stations, it should be evident that most of the earthquakes along the Zagros and Taurus/Bitlis tectonic zones are occurring in the upper crust (red circles) and to a much lesser extent in the lower crust (green circles) and upper mantle (blue circles). Events deeper than 100 km are rare in this region. In the case of the few events denoted by small white circles on the map, their depth estimates are not well constrained, and their magnitudes are either undefined or too small to be well detected by the distant NISN station. Additional data from the seismic networks in Saudi Arabia, Qatar, the United Arab Emirates (UAE) and Oman would constrain the solution and show that these events are shallow too.

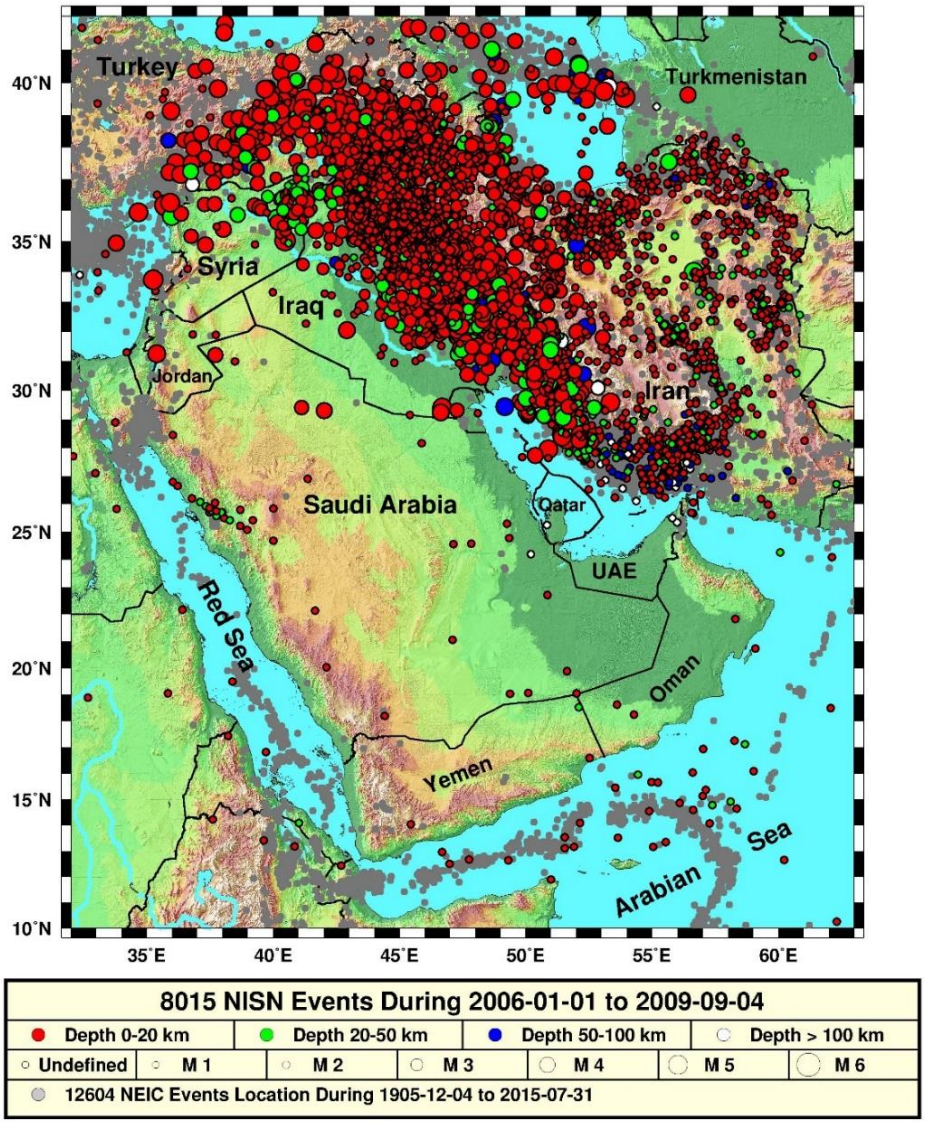

Figure-3: A composite seismicity map of the Arabian plate for the period 1905-2009. The NISN (8015) events for the period 2006/1/1-2009/9/4 color coded by depth and scaled by magnitude. The NISN events were located using NISN waveforms and neighboring countries' bulletins. The events reported by the NEIC (12604) and depicted in gray dots for the period 4/12/1905-31/7/2015 are included herein to delineate the boundaries of the Arabian plate.

Source Mechanism

Most of the seismic activity in the ME is confined to well-defined narrow zones that suggest strong correlation between the seismicity, the kinematics of the plate, and deformation patterns along its boundaries. This pattern of seismicity is a manifestation of the translational motion toward the northeast and the counterclockwise rotation of the Arabian plate as shown in *Figure: 2.*

The spatial distribution of earthquakes along the Zagros Mountain range defines an approximately 200 km wide and 1500 km long seismic belt. The seismic activity extends throughout the main thrust zone and folded

belt of the Zagros, and it appears to occur along a combination of normal, reverse or thrust and strike-slip faults. References *[8, 9, 34, 35, 36, 37, 38]* have all demonstrated that most of the events occur in the upper crust, and there are no evidences for the occurrence of mantle earthquakes beneath the Zagros, as suggested by *[39, 40]*. Their findings are well supported by the focal mechanism solutions of earthquakes located along the Zagros (*Figure: 4*).

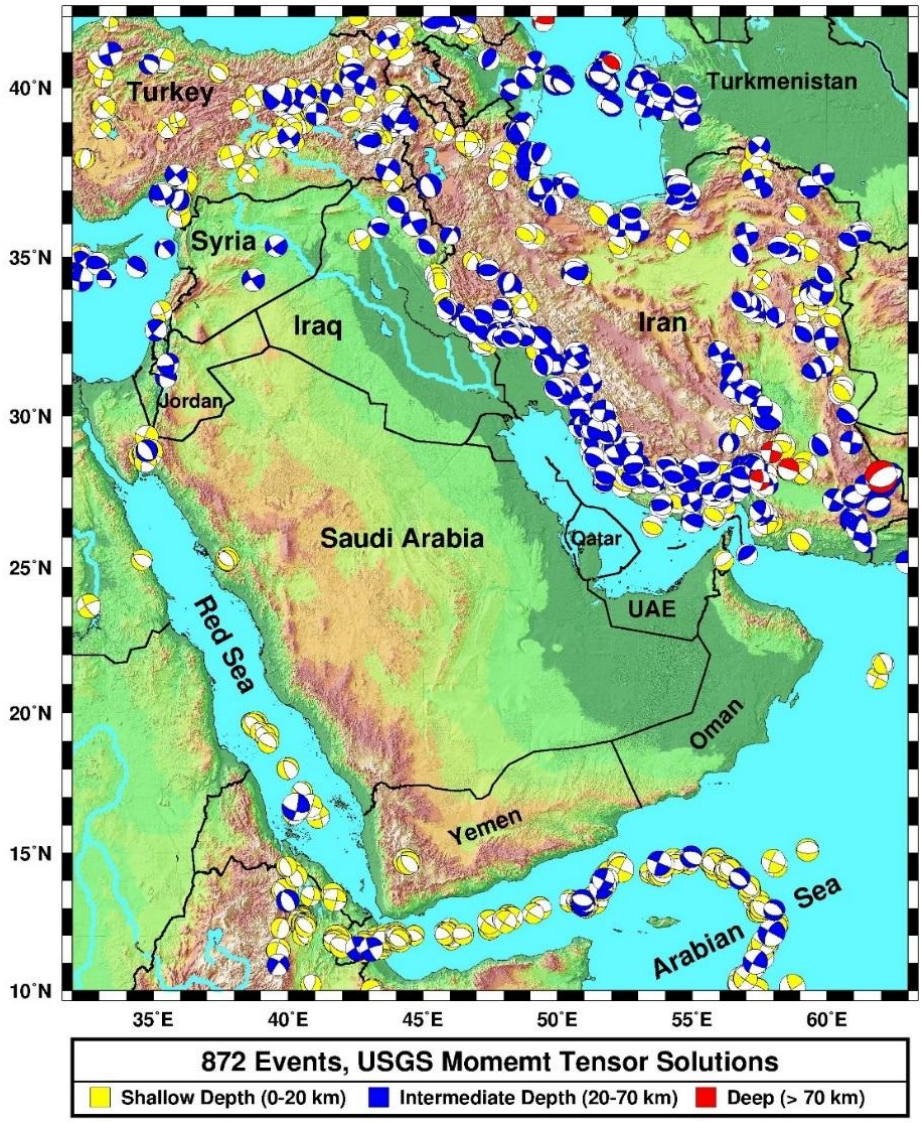

Figure-4: Fault mechanism solutions based on MT analysis of 872, mostly shallow, events with magnitude (*Mw* > 4.0) that occurred along the boundaries of the Arabian plate during 1976-2015.

The USGS Moment Tensor (MT) and Harvard University Centroid Moment Tensor (CMT) solutions presented in *Figure: 4* are for 872 earthquakes (Mw > 4.0) that occurred during 1976-2015. With a few exceptions the solutions also show that the majority of the earthquakes along the plate's boundaries are occurring within the crust (depth < 70 km) along the numerous normal, thrust and strike-slip faults in the region. The solutions are obtained using the moment tensor method for inverting teleseismic long-period waveforms, primarily Rayleigh and Love waves *[41]*. Furthermore, as part of the NISN routine data analysis process additional MT solutions for the larger events are being determined using the method in *[42*]. *Figure: 5* shows one such example of the focal mechanism of an event that occurred on 18/7/2009 at 34.85^{o}N and 43.35^{o}E near the town of Sharqat. According to the USGS, the event origin time is 20:32:27.6, depth of 7.4 km and *Mw*=5.2.

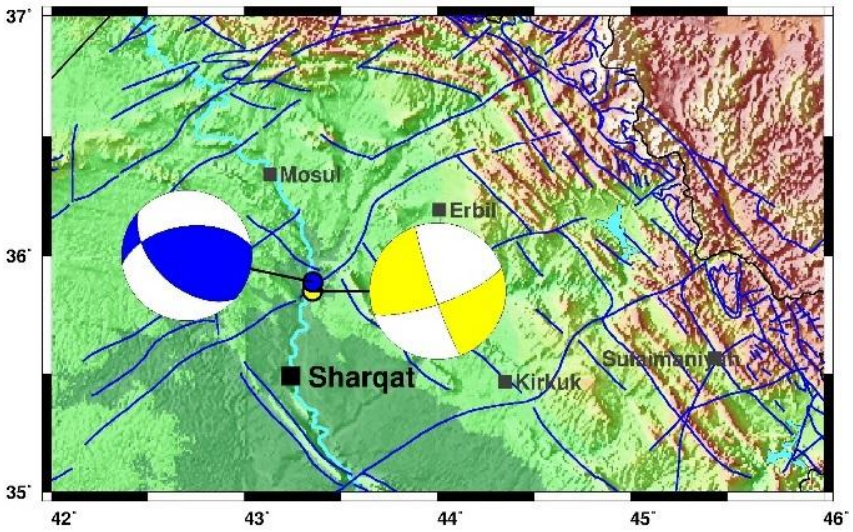

Figure-5: Sharqat event fault mechanism (yellow) determined using NISN (KSIRS/KI01) and GSN stations (CSS, MALT, RAYN, ANTO and GNI) data. The first nodal plane strike angle is 161°, dip 85° and rake of -165°; the second nodal plane strike angle is 70°, dip 75° and rake of -5°. The USGS/CMT solution is shown in blue. Both solutions indicate the event occurred in the upper crust at depths of 20 and 25.8 km, respectively. The blue lines represent the faults in the region.

Many earthquakes occur along the Red Sea and Gulf of Aden sea-floor spreading zones. They are mostly associated with the axial trough and transform faults, and they are of shallow depth. From fault plane solutions it is seen that the tensional stress field for the Red Sea and Gulf of Aden is directed toward the NE-SW.

Although small to moderate earthquakes are frequent along the Dead Sea transform fault system, *[43]* characterize the observed activity level during this century as a period of conspicuous seismic quiescence. Earthquake swarms, such as the one in the Gulf of Aqaba in 1983 *[44]* are known to occur. A recent example of an earthquake swarm occurred during 24/1/2015–10/2/2015 near the city of Sulaimaniyah in Kurdistan, Iraq. Based on NISN data, *Figure: 6* shows that more than 160 small earthquakes occurred along some of the faults in the region.

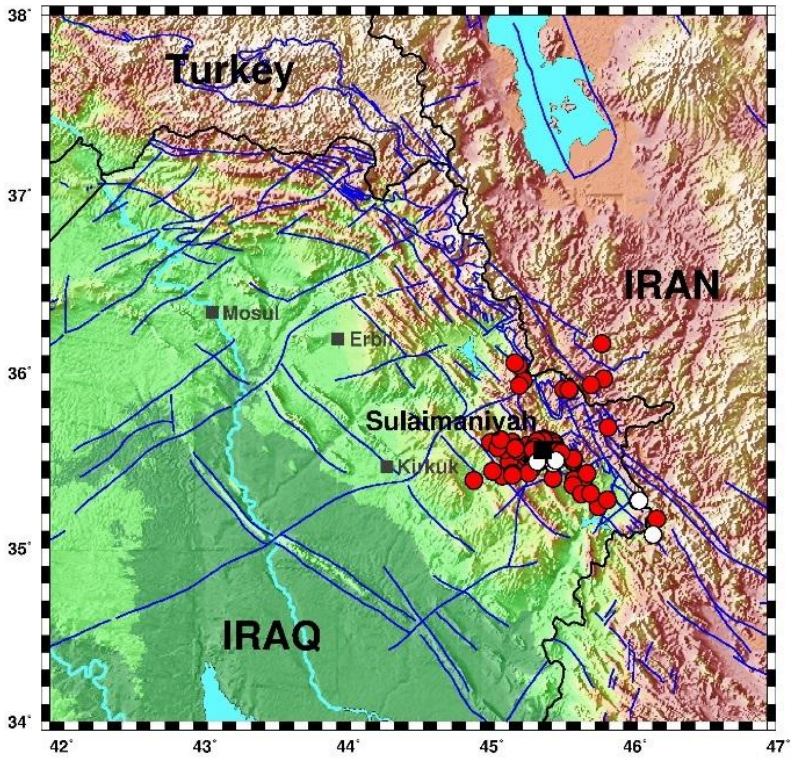

Figure-6: Sulaimaniyah earthquakes swarm of 24/1/2015-10/2/2015. The 160 NISN events are shown in red circles. The 7 Iranian bulletin events are shown in white circles with modified *mbLg* magnitude range of 2.5-3.6. The blue lines represent the faults in the region.

Crustal Structure

NISN is a network of 10 three-component broadband stations that since inception in 2006 have produced a wealth of high quality seismic waveform data sampled at 100 sps *[29]*. *Figure: 7A* illustrates the quality of an event's waveforms recorded at eight of the NISN stations, and on them the regional phases *Pn*, *Pg*, *Sn*, *Lg* and *Rg* are distinguishable. According to the NEIC, this event occurred on 26 December 2005 at 23:15:53.4, 49.1713°N, 49.2201°E, 32 km depth, and m_b=5.1. The epicentral distances and azimuths range from about 130-140 km and 2-5 degrees, respectively.

In the second example (*Figure: 7B*), the vertical component waveforms are shown from three events

recorded at station KSWW. They are presented to illustrate the influence of the Zagros tectonic structure on wave propagation. Numerous studies have shown that some of the regional phases (*e.g.*, *Sn* and *Lg*) can be attenuated or blocked from propagating across or along major tectonic structures. In *Figure: 7B* the top waveform, whose backazimuth is about 29°, exhibits discernable *Pn*, *Pg* and *Lg*, but no clear *Sn*, for crossing the Zagros-Bitlis zone, whereas the second waveform shows *Pn* and *Sn*, but no *Pg* or *Lg*, for traveling along the Zagros axis. In contrast, events with a propagation path to NISN stations from the west or south (bottom waveform) exhibit unobstructed propagation of *Pn*, *Pg*, *Sn* and *Lg* phases. As shown in *Figure: 8*, there is a pronounced difference in the waveforms and observed seismic phases arriving at the stations from different azimuths.

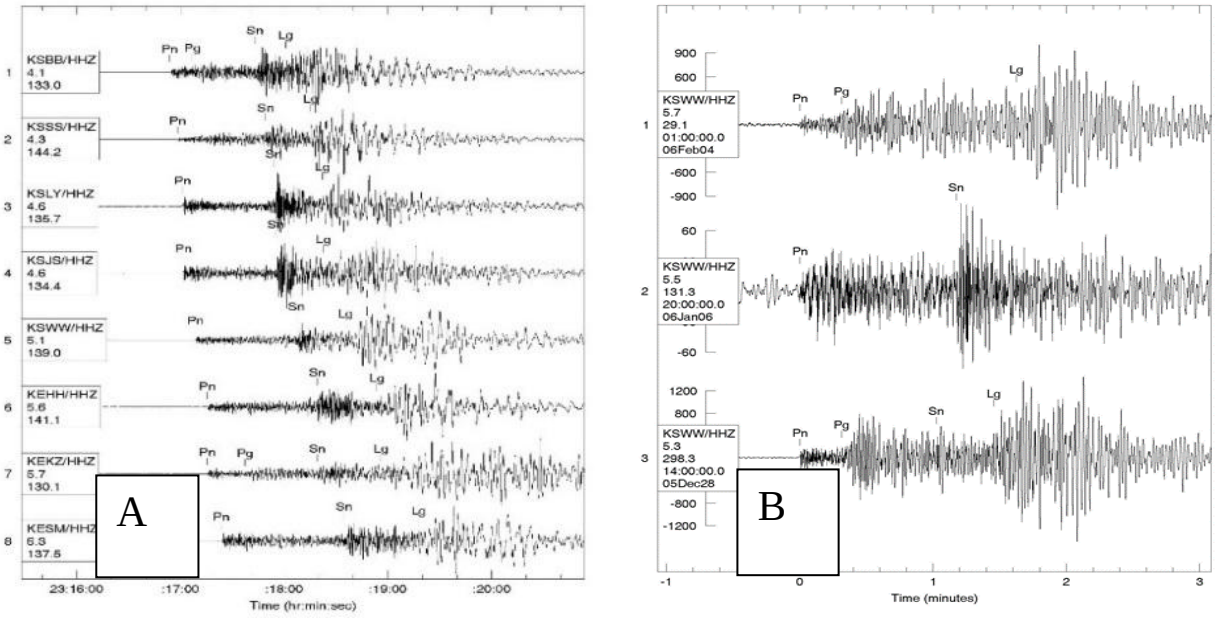

Figure-7: (A) Sample waveforms recorded at eight NISN stations showing the quality of recorded data and pronounced arrival of *Pn*, *Pg*, *Sn*, *Lg*, and *Rg* phases. (B) Waveforms from three events showing the impact of tectonic structures (in the form of attenuation or signal blockage) on wave propagation of various azimuths on regional phases like *Pn*, *Pg*, *Sn*, and *Lg*.

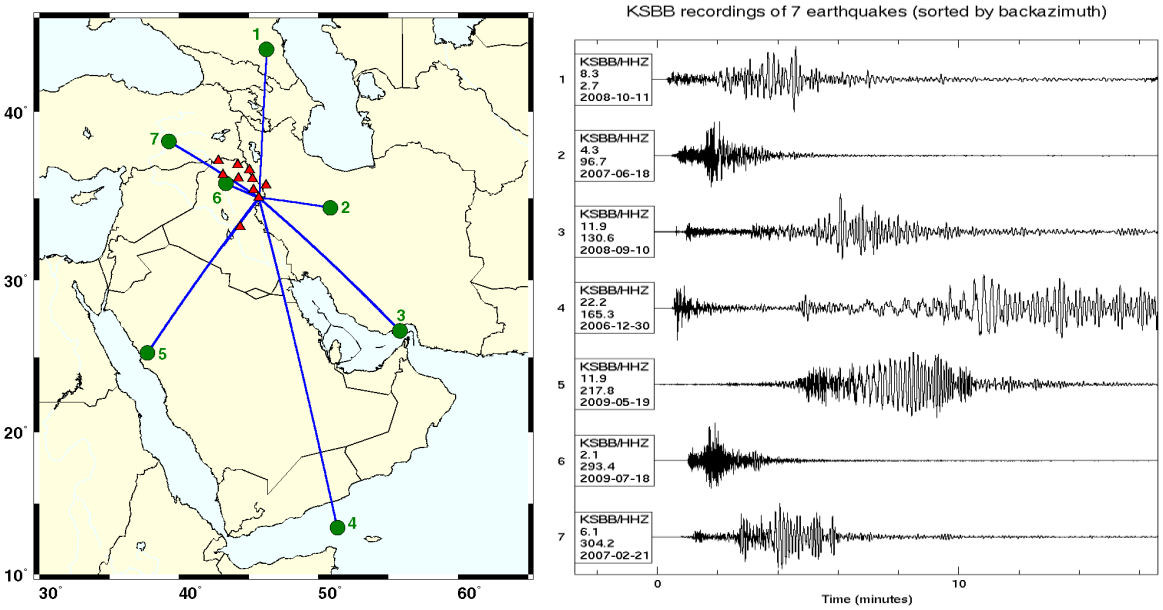

Figure-8: Example showing the impact of tectonic structures (in the form of attenuation or signal blockage) on wave propagation of various azimuths on regional waveforms.

The simplest way to estimate the depth to the major crustal discontinuities is to refer to the relationship between the onset time of observed seismic phase and epicentral distance as shown in *Figure: 9*. In this example based on the *Sn* and *Pn* crustal phases times, the Moho discontinuity is estimated to be about 45-47 km deep under the Zagros. The technique is applicable only to a small flat-layered region that exhibits little or no lateral and vertical variations. Otherwise, it provides an average estimate of the depth to the discontinuities.

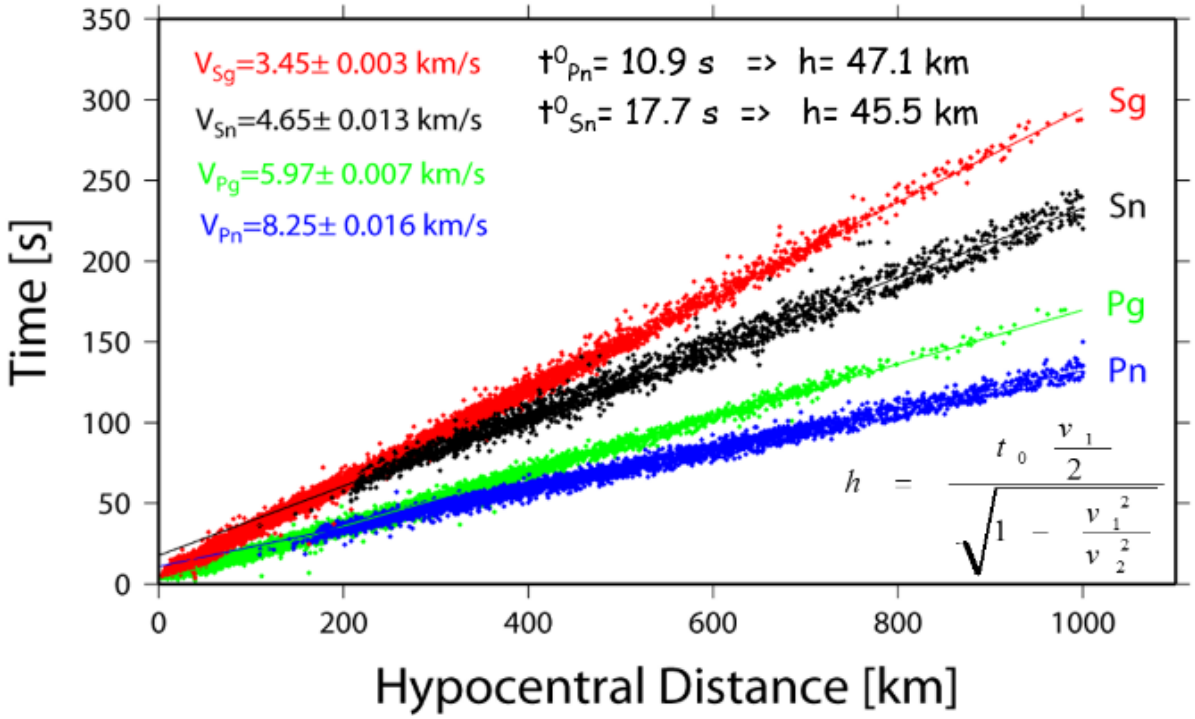

Figure-9: Estimated Moho discontinuity depth beneath the Zagros based on travel times of crustal phases.

1. Surface Wave Models

The dispersive property of Rayleigh and Love seismic surface waves provides a reliable way to map the seismic velocity structure of a region. Although the shear velocity models *[45]* estimated from the inversion of Rayleigh waves crossing more than one tectonic zone (*i.e.*, mixed-paths dispersion curves) show significant variation in the ME, the resulting average models are only marginally better than those obtained from the travel-time versus distance approach described above. To better understand the tectonic framework of the Arabian plate and surrounding regions, one needs to map the vertical and lateral variations of the crust and upper mantle structures. To quantitatively describe the lateral heterogeneity in the region, *[45]* used a Rayleigh wave group velocity regionalization approach to estimate the pure-path dispersion curves within the elements of a grid and then invert for a three-dimensional seismic shear velocity model for the ME. The grid-dispersion inversion method is an iterative stochastic inversion that represents a set of observed mixed-path dispersion curves as the sum of group delays (pure-path dispersion curves) within grid elements. Details of the regionalization principle and method can be found in *[46]*.

Among the advantages of grid-dispersion inversion are that the grid element size mainly depends on the dispersion information density and that the method requires no *a priori* assumption regarding either the surface or subsurface geology of a region. In formulating the inversion process, grids with various element sizes were used to test the coverage and resolution of the 152 mixed-path dispersion curves obtained from the records of stations TAB, SHI, EIL and JER. The adopted grid divides the region into 100 equal area elements. The dimension of each grid element is 3×3 degrees. The pure-path distances within the individual grid elements are then determined and normalized by their corresponding mixed-path distances in the kernel matrix. The starting group velocity values for each grid element are assumed to be the average of all group velocity measurements, and the theoretical slowness values are then calculated. Subsequently, the initial

dispersion curves for the individual grid elements are updated by the solution from the preceding iteration.

The estimated tomographic (three-dimensional) shear velocity structure of the region is presented in *Figure: 10*. It depicts the lateral velocity heterogeneity at depths of 5.0 km to 80.0 km, in 5.0 km increments. These isodepth surfaces are derived from the pure-path shear velocity models of the grid elements covering the region. The most striking feature of these maps is the continuous change in the distribution and location of the troughs and peaks of shear velocity at various depths. For instance, the velocity lows that are associated with the Mesopotamian foredeep seem to persist to about 30.0 km depth. Also, the influence of surface geology on the subsurface structure of the plate slowly diminishes with increasing depth. An important result of this analysis is the remarkable delineation of the Arabian shield and Mesopotamian foredeep by the shear velocity contours at 5.0 km and 10.0 km depths. The shape and extension of the contours correlate well with the physiographic boundaries and surface geology of these major tectonic units. The contours show that the exposed shield area is confined to the west and southwestern part of the plate, whereas the Mesopotamian foredeep exhibits northern, northwestern and western trends that are parallel to the Zagros mountain belt. At 5.0 km depth, the velocity within the shield reaches a high of 3.2 km/sec, and it drops to a low of 2.6-2.7 km/sec within the thick sedimentary column of the foredeep. At 10.0 km depth, the velocity high is 3.7 km/sec in the shield, and the velocity low is 3.2 km/sec in the foredeep. Also, the shear velocity of the shield area decreases rapidly toward the north and northeast, and it decreases gradually toward the east and south. The implication is that the observed velocity variation is in good agreement with the pattern of *[26]* depth contours to the top of the basement in the region.

Another important result involves the shear velocity variation within the upper and lower crust as well as the effect of the Mesopotamian sedimentary layer on the structure of the plate. At 15.0-25.0 km depth, the differences in shear velocity between the various tectonic regions decrease to approximately 0.3 km/sec. The higher velocities are observed under the shield, and the lower velocities are under the foredeep. Although this lateral velocity distribution is familiar, because it simply follows that of the shallower layers which are influenced by the configuration of the shield and foredeep structures, it is the depth at which this pattern can be observed that is interesting. The impact of the exceptionally thick sedimentary column of the foredeep can be observed to a depth of at least 30.0 km. In addition, the lateral velocity variation within the lower crust seems to increase from 0.3 km/sec to 0.4 km/sec at 40.0-45.0 km depth. The velocity under the shield is no longer higher than that under the foredeep. Instead, the highest shear velocities are observed beneath the northern and western regions of the plate. This marks a significant change with increasing depth in the lateral velocity heterogeneity of the Arabian plate structure. As indicated earlier, the shear velocity under the Arabian shield is higher than that under the Mesopotamian foredeep. Below 40.0 km the isodepth contours show a remarkable reversal in the pattern of shear velocity variation indicating that the velocity under the shield region is lower than that under the rest of the plate.

Similar to the isodepth surfaces, *Figure: 11* shows isovelocity contour maps of the region at 3.0, 3.5 and 4.0 km/sec. Comparison between these surfaces shows significant velocity variation with depth throughout the region. Also, the pattern of observed velocity heterogeneity correlates well with the major tectonic features. The contours primarily follow the structure and trend of the Arabian shield and Mesopotamian foredeep. Therefore, it is not surprising to observe that the 3.0, 3.5 and 4.0 km/sec velocities are found at shallower depth under the shield and at greater depths in the foredeep. This suggests that the lateral velocity distribution is influenced by the structural configuration of the thick sedimentary column of the foredeep.

Furthermore, the shield depth contours in *Figure: 10* show steeper gradient towards the north and northeast and a more gradual gradient to the east and southeast. This is in agreement with *[26]* depth contours to the top of the basement. Also, the depth contours indicate that the crustal structure of the Arabian plate increases in thickness towards the north, northeast, east and southeast as the distance away from the shield increases. In other words, the crust is thicker under the foredeep and thinner under the shield.

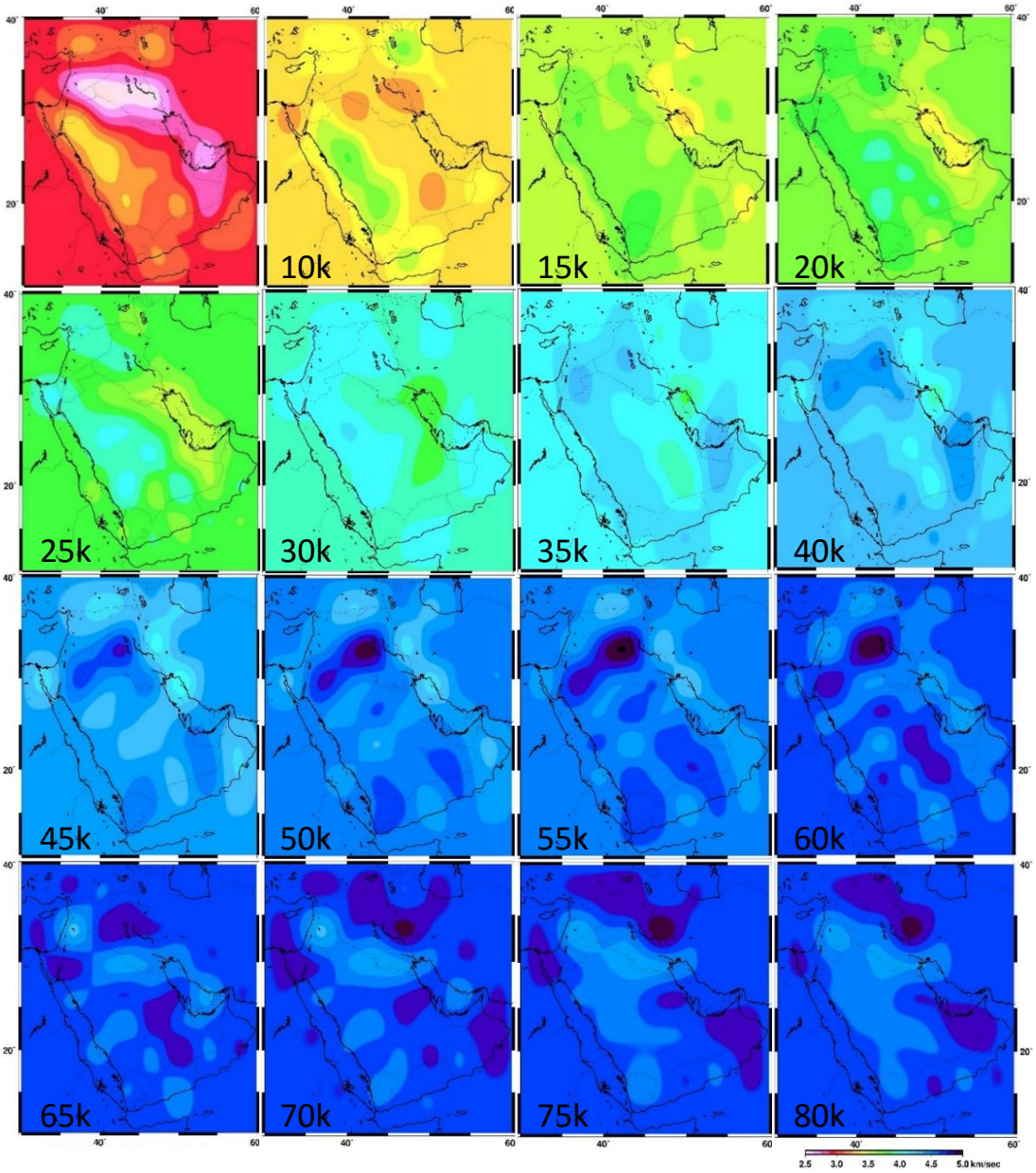

Figure-10: Tomographic images of the Arabian plate showing the shear velocities variation at given depths.

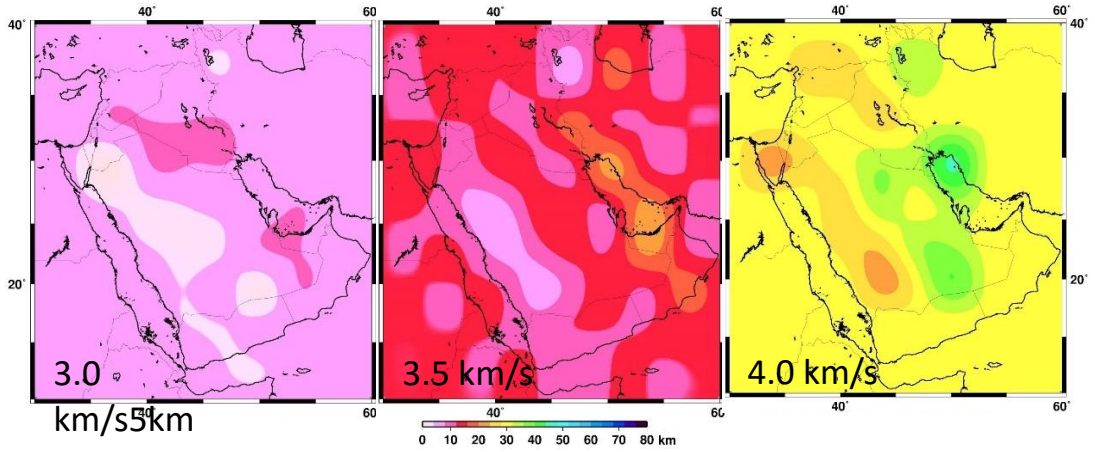

Figure-11: Tomographic images of the Arabian plate showing the depth variation for given shear velocities.

2. Body Wave Models

Estimating the seismic velocity structure beneath NISN stations provides an independent means to constrain and maybe improve the velocity models obtained from other inversion techniques and modeling approaches. Toward this end the well-known Receiver Function (RF) inversion technique is applied to teleseismic *P* wave data recorded at some of the NISN stations (*Figure: 12*). RF are time series computed from three-component seismograms that show the relative response of earth structure near a receiver *[47]*. The RF methodology has been extensively used by seismologists. While the overall method is straightforward to define, the computation of reliable receiver functions can be problematic due to the non-uniqueness of RF inversions, a topic that has been the subject of extensive research, *e.g., [48, 49, 50, 51, 52, 53, 54]*. Through these efforts, many improvements to the technique have been developed to overcome difficulties stemming from instabilities in the deconvolution process.

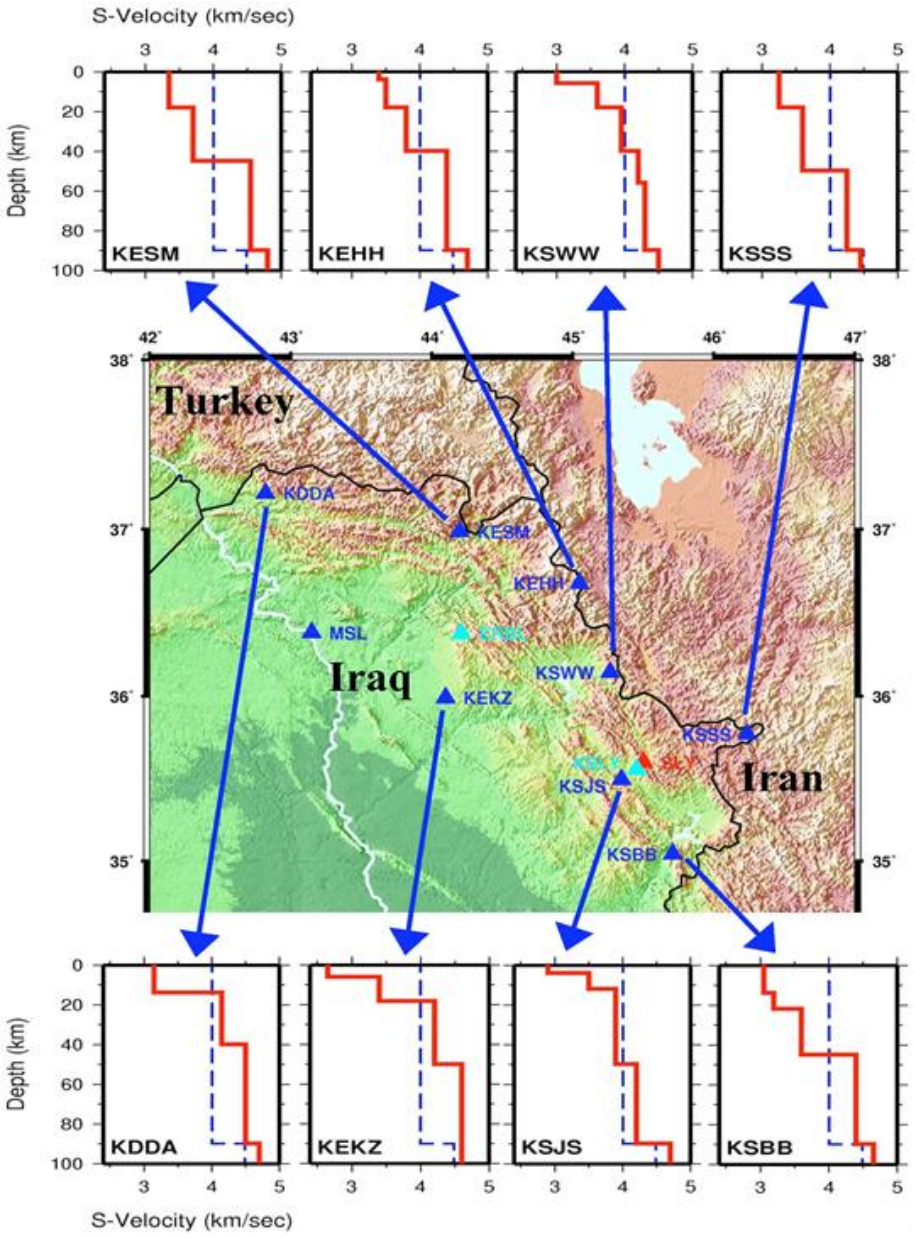

Figure-12: Locations of NISN stations (blue triangles) and associated shear wave velocity models obtained from the RF inversion. The Moho depths beneath the stations in the foothills appear shallower than those beneath the stations in the Zagros Mountains. Similarly, a mid-crustal velocity increase appears at shallower depth below the foothills (~ 15 km depth) compared to the Zagros Mountains (~ 20 km depth). Temporary stations ERBL and KSLY are depicted in aqua triangles, and SLY in red triangle.

In this study, *[42, 47]* computational algorithms are used to determine the RF and invert for the seismic velocity models, but without the benefit of utilizing surface waves (an invaluable step being pursued as more data become available).

A search of the Preliminary Determination of Epicenters (PDE) bulletin for the period from 30 November 2005 to 31 August 2006 resulted in a list of teleseismic events at various azimuths and epicenteral distances in the range of 30-90 degrees from NISN. A similar search of the NISN data resulted in about 150 events (4500 waveforms) with magnitudes of 5.5 and larger that were scrutinized for the RF analysis. The quality of the observed *P* waves was assigned a subjective grading scale (A-good through D-poor) to reflect the quality of the waveforms' signal to noise levels (*i.e.*, acceptable level of signal-to-noise ratio to produce stable and reliable receiver functions). Only grade A and B waveforms were used in this study.

Following reformatting of the data to include the required event location (latitude, longitude, and depth) and *P* wave arrival time in the Seismic Analysis Code (SAC) header *[58]*, the RF were estimated for each station record. Also in preparation for the inversion process a multi-layered initial shear velocity model was created following the general characteristics of the models derived by *[45]* using the Rayleigh waves group velocity dispersion curves for paths traversing the study area. The shear velocity of the crustal layers was set to 4.0 km/sec and the upper mantle layers (below 90 km) to 4.5 km/sec (blue dashed line in *Figure: 12*). The thicknesses of the layers vary from 0.5 km at the top and gradually increased with depth to a maximum of 10 km at the bottom of the crust. The thicknesses of the layers in the upper mantle were set to 10-100 km.

The RF inversion process is iterative and requires a certain measure of damping to constrain the model. The resulting one-dimensional seismic velocity models under the NISN stations KESM, KEHH, KSWW, KSSS, KDDA, KEKZ, KSJS and KSBB are presented in *Figure: 12*. No models were estimated for stations MSL and BHD due to the scarcity of data and low signal-to-noise ratios that disqualified most of the available waveforms recorded at these two stations. Common among the eight models is the relatively lower than average shear velocities of the layers when compared with other regions of the Earth, and the presence of a pronounced discontinuity at about 15 km depth. The depth of the Moho seems to vary from about 45-55 km. These findings are consistent with previous studies by, among others, *[33, 45, 55]*. Also noticeable is the diminishing data resolution at depths exceeding about 80km. The observed change in shear velocity values below that depth is simply a perturbation in response to the better estimated velocities of the crustal layers where the data resolution is highest.

Conclusions

Understanding the geologic evolution and geophysical characteristics of a region has economic and social implications far beyond just academic research. The Arabian plate and surrounding regions have had their share of devastating earthquakes in the past. Numerous faults and dormant volcanic activities should serve as a reminder of what could happen when a moderate to large earthquake occurs in this region. Hence, the subject of this study is to better understand the seismicity and crustal seismic velocity structure of the Arabian plate. In summary, the inferred conclusions are:

1. Most of the interplate and intraplate earthquakes in the region occur at shallow depth. This is supported by the events' relocation and by MT analysis results. With the events' being concentrated in the crust, this suggests that the boundary between the Arabian plate and Iranian and Turkish plateaus is still in an early stage of continental collision in which tectonic activity is still shallow and has not yet progressed to the stage at which deeper seismicity would be characteristic of under thrusting.
2. The observed surface waves exhibit well developed and dispersed fundamental and higher modes waveforms. Events whose paths traverse the Mesopotamian foredeep show remarkable sinusoidal fundamental-mode surface waves that are characteristic of sedimentary basins. The mixed-path Rayleigh wave group velocity is found to be as low as 1.92 km/sec at 3.0 sec period, and the highest group velocity is found to be 3.87 km/sec at 68 sec. The first higher-mode velocities are found to

vary between 2.74 km/sec and 4.46 km/sec over a period range of 3-21 sec. In general, these velocities are noticeably lower than values obtained for other regions of the earth.

3. The models obtained from the inversion of mixed-path dispersion curves suggest that the velocity structure of the Arabian plate is characterized by a relatively thick, 5-15 km, sedimentary layer. The models also suggest the Conrad and Moho discontinuities vary in depth between 15-20 km and 37-45 km, respectively. The crust is thinner under the shield and thicker under the Mesopotamian foredeep. The shear velocities within these layers vary over a wide range, depending on the tectonic provinces their paths traverse.
4. The estimated three-dimensional model shows significant lateral and vertical velocity variations, and it correlates well with the major tectonic features of the plate. The model clearly delineates the boundaries of the Arabian shield and extension of the Mesopotamian foredeep. Near the surface, *i.e.*, at 5 km depth, the shear velocity within the shield reaches 3.2 km/sec, and it drops to approximately 2.6 km/sec within the Mesopotamian foredeep. At a depth of 25 km, the difference in velocity between these major tectonic provinces decreases to 0.3 km/sec, indicating less spatial variation in the lower than upper crust of the Arabian plate. Also, the pattern of velocity and depth contours estimated from the three-dimensional model shows agreement with *[26]* tectonic map for the region.
5. Although the three-dimensional model shows that the crustal velocities for the shield region are generally higher than the rest of the plate, a clear reversal in the lateral velocity distribution is observed below 40.0 km depth. While the shear velocity under the shield decreases with increasing depth, it gradually increases under the foredeep. This may suggest that a low-velocity zone exists underneath the shield but not under the foredeep.

Acknowledgments

Acknowledgements are due to Mathew Sibol, Roland Gritto, Robert Wagner, Adam Sargent, and Yajun Wang for analyzing the data. Wilmer Rivers and Florence Martin are appreciated for reviewing and editing the text.

Acknowledgements are also due to Borhan Salih, Shaho Abdullah, Ali Abdulkhaliq, Basoz Ali, Layla Omar, Nokhsha Aziz, Nian Hama, Mohammed Ismael, Hemin Hashm, Dasne Taha, Sangar Ali, Beston Sherzad, Delan Tahsen, Sakar Mohammed, Zardasht, Omar, Abdulaziz Salim and Hamed Hassan for helping with maintaining the stations and collecting the NISN data; Rashid Zand, Mohammed Abdul Rahman, Omed Mohammed Mahsum and Dara Hassan for their administrative support.

The maps in this article were created using the Generic Mapping Tools *[57]*, and the Seismic Analysis Code (SAC) *[58]* and the Geotool waveform measurement software were used to plot the waveform.

References

[1] Adams, R. D., and M. Barazangi (1984). Seismotectonics and seismology in the Arab region: A brief summary and future plans, *Bull. Seism. Soc. Am.* **74**: 1011-1030.

[2] Jackson, J., and D. McKenzie (1984). Active tectonics of the Alpine-Himalayan belt between western Turkey and Pakistan, *Geophys. J. R. astr. Soc.* **77**, 185-264.

[3] Stocklin, J. (1974). Possible ancient continental margins in Iran, in *Geology of Continental Margins*, edited by C. Burk and C. Drake, Springer-Verlag, New York, 873-877.

[4] Sengor, A. M. C. and W. Kidd (1979). Post-collisional tectonics of the Turkish-Iranian plateau and a comparison with Tibet, *Tectonophysics* **55**, 361-376.

[5] Falcon, N. L. (1967). The geology of the northeastern margin of the Arabian basement shield, *Adv. Sci.* **24**, 31-42.

[6] Ala, M. (1974). Salt diapirism in southern Iran, *Am. Assoc. Pet. Geol.* **58**, 1758-1770.

[7] Stocklin, J. (1968). Structural history and tectonics of Iran: a review, *Bull. Am. Assoc. Pet. Geol.* **52**, 1229-1258.

[8] Jackson, J. (1980). Errors in focal depth determination and the depth of seismicity in Iran and Turkey, *Geophys. J. R. astr. Soc.* **61**, 285-301.

[9] Jackson, J., and T. J. Fitch (1979). Seismotectonic implications of relocated aftershock sequences in Iran and Turkey, *Geophys. J. R. astr. Soc.* **57**, 209-229.

[10] Berberian, M. (1981). Active faulting and tectonics of Iran, *A.G.U. Geodynamic Series* **3**, 33-69.

[11] Jackson, J., and D. McKenzie (1984). Active tectonics of the Alpine-Himalayan belt between western Turkey and Pakistan, *Geophys. J. R. astr. Soc.* **77**, 185-264.

[12] McKenzie, D. P., D. Davies, and P. Molnar (1970). The plate tectonics of the Red Sea and East Africa, *Nature* **226**, 243-248.

[13] Whiteman, A. J. (1970). The existence of transform faults in the Red Sea depression, *Phil. Trans. Roy. Soc. London* **A 267**, 407-408.

[14] Ross, D., and J. Schlee (1973). Shallow structure and geologic development of the southern Red Sea, *Bull. Geol. Soc*. **84**, 3827-3848.

[15] Girdler, R. W., and P. Styles (1974). Two-stage Red Sea floor spreading, *Nature* **247**, 7-11.

[16] Le Pichon, X., and J. Francheteau (1978). A plate-tectonic analysis of the Red Sea-Gulf of Aden area, *Tectonophysics* **46**, 369-406.

[17] Cochran, J. R. (1981). The Gulf of Aden: structure and evolution of a young ocean basin and continental margin, *J. Geophys. Res.* **86**, 263-287.

[18] Freund, R. (1965). A model of the structural development of Israel and adjacent areas since Upper Cretaceous times, *Geol. Mag.* **102**, 189-205.

[19] Freund, R., Z. Garfunkel, I. Zak, M. Goldberg, T. Weissbrod, and B. Derin (1970). The shear along the Dead Sea rift, *Phil. Trans. Roy. Soc. London* **A 267**, 107-130.

[20] Ben-Menahem, A., A. Nur, and M. Vered (1976). Tectonics, Seismicity and structure of the Afro-Eurasian junction - The braking of an incoherent plate, *Phys. Earth Planet. Int.* **12**, 1-50.

[21] Nur, A. and Z. Ben-Avraham (1978). The eastern Mediterranean and the Levant: tectonics of continental collision, *Tectonophysics* **46**, 297-311.

[22] Ben-Avraham, Z., Z. Garfunkle, G. Almagro, and J. K. Hall (1979). Continental breakup by leaky transform: the Gulf of Elat (Aqaba). *Science* **206**, 214-216.

[23] Garfunkle, Z., I. Zak, and R. Freund (1981). Active faulting in the Dead Sea rift, *Tectonophysics* **80**, 1-26.

[24] Zak, I., and R. Freund (1981). Asymmetry and basin migration in the Dead Sea rift, *Tectonophysics* **80**, 27-38.

[25] Neumann Van Padang, M. (1963). Catalogue of the active volcanoes and solfatar fields of Arabia and the Indian Ocean, Part 16, in Catalogue of the Active Volcanoes of the World, edited by the International Association of Volcanology.

[26] Brown, G. F. (1972). *Tectonic map of the Arabian Peninsula*, Scale 1:4000000, U.S. Geologic Survey.

[27] Reilinger, R., *et al.*, (2006). GPS constraints on continental deformation in the Africa-Arabia-Eurasia continental collision zone and implications for the dynamics of plate interactions, *J. Geophys. Res.* **111**, B05411, doi:10.1029/2005JB004051.

[28] Reilinger, R. F. (2009). Seismotectonics of the Arabian Plate and its boundaries III, *EOS Trans AGU*, 90 (52), Fall Meeting Suppl. Abstract T54C-2011.

[29] Ghalib, H. A. A., G. I. Aleqabi, B. S. Ali, B. I. Saleh, D. S. Mahmood, I. N. Gupta. R. A. Wagner, P. J. Shore, A. Mahmood, S. Abdullah, O. K. Shaswar, F. Ibrahim, B. Ali, L. Omar,

N.I. Aziz, N. H. Ahmed, A. A. Ali, A.-K. A. Taqi, and S. R. Khalaf (2006). Seismic characteristics of Northern Iraq and surrounding regions, in *Proceedings of the 28th Seismic Research Review: Ground-Based Nuclear Explosion Monitoring Technologies*, pp. 40-48.

[30] Ghalib, H. A. A., G. Aleqabi, E. Al-Tarazi, T. Al-Yazjeen, O. Ahmed, B. S. Ali, K. Qadir and A. Ali (2012). A proposal to establish a Middle East seismographic network, 7th Gulf Seismic Forum, Jeddah, Saudi Arabia.

[31] Fadhil I. Khudhur and H. A. A. Ghalib (2015). Open Invitation to Join the virtual Middle East Seismographic Network (vMESN), *Proposal Submitted to Participants of the Arab League's Permanent Committee for Meteorology 31 Session*, Jeddah, Kingdom of Saudi Arabia, April 26-30.

[32] Ghalib, H. A. A., D. R. Russell, and A. Kijiko (1985). Optimal design of a seismological network for the Arabian countries, *Pure appl. Geophys.* **122**: 694-712.

[33] Pasyanos, M. E., W. R. Walter, M. Flanagan, P. Goldstein, and J. Bhattacharyya (2004). Building and testing *a priori* geophysical model for western Eurasia and North Africa, *Pure Appl. Geophys*. **166**, p. 47.

[34] Niazi, M., I. Asudeh, G. Bullard, J. Jackson, G. King, and D. McKenzie (1978). The depth of seismicity in the Kermanshah region of the Zagros Mountains (Iran), *Earth Planet. Sci. Lett.* **40**, 270-274.

[35] Berberian, M. (1979). Evaluation of the instrumental and relocated epicenters of Iranian earthquakes, *Geophys. J. R. astr. Soc.* **58**, 625-630.

[36] Jackson, J., and T. Fitch (1981). Basement faulting and the focal depths of the larger earthquakes in the Zagros Mountains (Iran), *Geophys. J. R. astr. Soc.* **64**, 561-586.

[37] Kadinsky-Cade, K., and M. Barazangi (1982). Seismotectonics of southern Iran: the Oman line, *Tectonics* **1**, 389-412.

[38] Asudeh, I. (1983). I.S.C. mislocation of earthquakes in Iran and geometrical residuals, *Tectonophysics* **95**, 61-74.

[39] Nowroozi, A. A. (1971). Seismotectonics of the Persian Plateau, eastern Turkey, Caucasus, and Hindu-Kush regions, *Bull. Seism. Soc. Am.* **61**, 317-341.

[40] Nowroozi, A. A. (1972). Focal mechanism of earthquakes in Persia, Turkey, West Pakistan, and Afghanistan and plate tectonics of the Middle East, *Bull. Seism. Soc. Am.* **62**, 832-850.

[41] Dziewonski, A.M., Chou, T.-A., Woodward, J.H. (1981). Determination of earthquake source parameters from waveform data for studies of global and regional seismicity. *J. Geophys. Res.* **86**, 2825–2852.

[42] Herrmann, R. B. (2006). *Computer Programs in Seismology*, *Ver. 3.30*, Saint Louis University, St. Louis, MO. Web page: http://www.eas.slu.edu/People/ RBHerrmann/CPS330.html.

[43] Ambraseys, N. N., and M. Barazangi (1989). The 1759 earthquake of the Bekaa valley: Implications for earthquake hazard assessment in the eastern Mediterranean region, *J. Geophys. Res.* **94**, 4007-4013.

[44] El-Isa, Z. H., H. M. Merghelani, and A. Al-Shanti (1984). The Gulf of Aqaba earthquake swarm of 1983 January-April, *Geophys. J. R. astr. Soc.* **78**, 711-722.

[45] Ghalib, H. A. A., *Seismic velocity structure and attenuation of the Arabian plate*, Ph. D. Dissertation, Saint Louis University, Saint Louis, MO, p. 314, 1992.

[46] Feng, C. C., and T. L. Teng (1983). Three-dimensional crust and upper mantle structure of the Eurasian continent, *J. Geophys. Res.* **88**, 2261-2272.

[47] Ammon, C. J. (2006). Receiver-Function Analysis, Pennsylvania State University, University Park, PA. Web page: http: //eqseis.geosc.psu.edu/~cammon/HTML/ RftnDocs/rftn01.html.

[48] Burdick, L. J., and C. A. Langston (1977). Modeling crustal structure through the use of converted phases in teleseismic body-wave forms, *Bull. Seism. Soc. Am*, **67**, 677-691.

[49] Langston, C. A. (1977). The effect of planar dipping structure on source and receiver responses for constant ray parameter, *Bull. Seism. Soc. Am.* **67**, 1029-1050.

[50] Ammon, C. J. (1991). The isolation of receiver effects from teleseismic P waveforms, *Bull. Seism. Soc. Am.* **81**, 2504-2510.

[51] Cassidy, J. F. (1992). Numerical experiments in broadband receiver function analysis, *Bull. Seism. Soc. Am.* **82**, 1453-1474.

[52] Ligorría, J. P. and C. J. Ammon (1999). Iterative deconvolution and receiver-function estimation, *Bull. Seism. Soc. Am.* **89**, 1395-1400.

[53] Park, J. and V. Levin (2000). Receiver functions from multiple-taper spectral correlation estimates, *Bull. Seism. Soc. Am*. **90**, 1507-1520.

[54] Helffrich, G. (2006). Extended-time multitaper frequency domain cross-correlation receiver-function estimation, *Bull. Seism. Soc. Am.* **96**, 344-34.

[55] Aleqabi, G., M. Wysession, H. A. A. Ghalib, M. Sibol, B. Saeed Ali, B. Saleh, A. Mahmood, S. Abdullah, L. Omar, N. Aziz, N. Ahmed, D. Mahmood, N. Alridaha, T. Alnasiry, O. Shaswar, A. Ali, A. Taqi, S. Khalaf, F. Ibrahim (2007). Seismic velocity structure of Iraq and surrounding regions from surface-waves waveform inversion, (Abstract) *Seism. Res. Let.*, **78**, 310.

[56] Pasyanos, M. E., W. R. Walter, M. Flanagan, P. Goldstein, and J. Bhattacharyya (2004). Building and testing *a priori* geophysical model for western Eurasia and North Africa, *Pure Appl. Geophys*. **166**, p. 47.

[57] Wessel, P., and W. H. F. Smith, (1998). New, improved version of Generic Mapping Tools released, *EOS Trans. Amer. Geophys. U.*, vol. 79 (47), pp. 579.

[58] Goldstein, P. (1996). SAC2000; seismic signal processing and analysis tools for the century, *Seismological Research Letters*, **67**(2).